Carbon Clusters Containing Two Metal Atoms: Structures, Growth Mechanism, and Fullerene Formation

Konstantin B. Shelimov and Martin F. Jarrold*

Contribution from the Department of Chemistry, Northwestern University, 2145 Sheridan Rd., Evanston, Illinois 60208

Received September 6, 1995[⊗]

Abstract: Gas phase ion mobility measurements have been used to probe the structures and interconversion of $La_2C_n^+$ ($n = 1-100$) isomers. The smallest $La_2C_n^+$ clusters ($n \leq 10$) appear to be planar rings. However, planar mono- and bicyclic rings (the dominant isomers for C_n^+ and LaC_n^+, $n \leq 30$, clusters) are not observed for the larger $La_2C_n^+$ species. Instead, isomers which appear to be three-dimensional ring complexes dominate for unannealed $La_2C_n^+$ ($n \geq 17$) clusters. The formation of these complexes is probably driven by electrostatic forces. For $n \geq 30$ the three-dimensional ring complexes isomerize into metallofullerenes (and metal-containing graphite sheets for $n = 30-37$). The estimated activation energies for these isomerization processes are about 1 eV lower than those estimated for similar processes for planar C_n^+ and LaC_n^+ rings. Metallofullerenes with two non-endohedral metal atoms (for $n = 28-29$), one endohedral metal atom (for $n = 31-100$), and two endohedral metal atoms (for $n \geq 64$, only even n), are identified. Fullerene derivatives (presumably fullerene + ring complexes) are abundant in the unannealed isomer distributions for $La_2C_n^+$ ($n \geq 50$) clusters, but readily isomerize into regular fullerenes upon collisional heating.

Introduction

Endohedral metallofullerenes (fullerene cages encapsulating metal atoms) may provide many interesting and potentially useful applications, such as a high-temperature isolation of unstable species or an assembly of novel layered materials. A wide research effort is currently devoted to the production and characterization of these species.[1] To date, only a few metallofullerenes, such as $M@C_{82}$ (M = Y, La), have been obtained in macroscopic amounts in a sufficiently pure form for subsequent analysis.[2] These fullerenes have been studied with a variety of analytical techniques[3−6] and are the best-characterized metallofullerene species. Less is known about metallofullerenes containing multiple metal atoms. Most of the studies of these species reported so far have been performed on mixtures of several metallofullerenes containing Sc or Y.[4,6−10] Significant progress has recently been made in the purification of some Sc_2C_n metallofullerenes.[10,11] Of the species containing multiple La atoms, La_2C_{80} has been found to be the most prominent extractable metallofullerene,[12] and small amounts of La_2C_{72} have been isolated by HPLC.[13] Despite the recent advances, difficulties in the separation of fullerenes of different sizes and the generally low yields of M_nC_m metallofullerens still impede the progress in this field. A better understanding of structures, stabilities, and formation efficiencies of a wide range of metallofullerenes can be achieved by studying these species in the gas phase. Such studies can also provide information about non-fullerene isomers and help to identify metallofullerene precursors.

Ion mobility measurements are currently the most direct method for the analysis of the structures of medium-size clusters in the gas phase.[14] The method is based on the fact that the mobility of a cluster ion in a buffer gas depends on its shape. Ion mobility studies of the structures of a wide range of C_n^+ [15] and MC_n^+ (M = La,[16−19] Nb[20]) clusters have been reported

[⊗] Abstract published in *Advance ACS Abstracts,* January 15, 1996.

(1) For a recent review see: Bethune, D. S.; Johnson, R. D.; Salem, J. R.; de Vries, M. S.; Yannoni, C. S. *Nature* **1993**, *366*, 123.

(2) Chai, Y.; Guo, T.; Jin, C.; Haufler, R. E.; Chibante, L. P. F.; Fure, J.; Wang, L.; Alford, J. M.; Smalley, R. E. *J. Phys. Chem.* **1991**, *95*, 7564.

(3) Johnson, R. D.; de Vries, M. S.; Salem, J. R.; Bethune, D. S.; Yannoni, C. S. *Nature* **1992**, *355*, 239.

(4) Weaver, J. H.; Chai, Y.; Kroll, G. H.; Jin, C.; Ohno, T. R.; Haufler, R. E.; Guo, T.; Alford, J. M.; Conceicao, J.; Chibante, L. P. F.; Jain, A.; Palmer, G.; Smalley, R. E. *Chem. Phys. Lett.* **1992**, *190*, 460.

(5) Soderhom, L.; Wurz, P.; Lykke, K. R.; Parker, D. H.; Lytle, F. W. *J. Phys. Chem.* **1992**, *96*, 7153.

(6) Park, C.-H.; Wells, B. O.; DiCarlo, J.; Shen, Z.-X.; Salem, J. R.; Bethune, D. S.; Yannoni, C. S.; Johnson, R. D.; de Vries, M. S.; Booth, C.; Bridges, F.; Pianetta, P. *Chem. Phys. Lett.* **1993**, *213*, 196.

(7) Yannoni, C. S.; Hoinkis, M.; de Vries, M. S.; Bethune, D. S.; Salem, J. R.; Crowder, M. S.; Johnson, R. D. *Science*. **1992**, *256*, 1191. Shinohara, H.; Sato, H.; Ohkohchi, M.; Ando, Y.; Kodama, T.; Shida, T.; Kato, T.; Saito, Y. *Nature* **1992**, *357*, 52.

(8) Shinohara, H.; Sato, H.; Saito, Y.; Ohkohchi, M.; Ando, Y. *J. Phys. Chem.* **1992**, *96*, 3571.

(9) Shinohara, H.; Hayashi, N.; Sato, H.; Saito, Y.; Wang, X.-D.; Hashizume, T.; Sakurai, T. *J. Phys. Chem.* **1993**, *97*, 13438.

(10) Beyers, R.; Kiang, C.-H.; Johnson, R. D.; Salem, J. R.; de Vries, M. S.; Yannoni, C. S.; Bethune, D. S.; Dorn, H. C.; Burbank, P.; Harich, K.; Stevenson, S. *Nature* **1994**, *370*, 196.

(11) Shinohara, H.; Yamaguchi, H.; Hayashi, N.; Sato, H.; Ohkohchi, M.; Ando, Y.; Saito, Y. *J. Phys. Chem.* **1993**, *97*, 4259.

(12) Alvarez, M. M.; Gillan, E. G.; Holczer, K.; Kaner, R. B.; Min, K. S.; Whetten, R. L. *J. Phys. Chem.* **1991**, *95*, 10561.

(13) van Loosdrecht, P. H. M.; Johnson, R. D.; Beyers, R.; Salem, J. R.; de Vries, M. S.; Bethune, D. S.; Burbank, P.; Haynes, J.; Glass, T.; Stevenson, S.; Dorn, H. C.; Boonman, M.; van Bentum, P. J. M.; Meijer, G. In *Recent Advances in the Chemistry and Physics of Fullerenes and Related Materials*; Proceedings of the Symposium of the Electrochemical Society; Kadish, K. M., Ruoff, R. S., Eds.; The ECS: Pennington, NJ, 1994; p 1320.

(14) Hagen, D. F. *Anal. Chem.* **1979**, *51*, 870. Karpas, Z.; Cohen, M. J.; Stimac, R. M.; Wernlund, R. F. *Int. J. Mass Spectrom. Ion Proc.* **1986**, *83*, 163. von Helden, G.; Hsu, M. T.; Kemper, P. R.; Bowers, M. T. *J. Chem. Phys.* **1991**, *95*, 3835. For a recent review see: St. Louis, R. H.; Hill, H. H. *Crit. Rev. Anal. Chem.* **1990**, *21*, 321.

(15) von Helden, G.; Hsu, M. T.; Gotts, N. G.; Bowers, M. T. *J. Phys. Chem.* **1993**, *97*, 8182.

(16) Clemmer, D. E.; Shelimov, K. B.; Jarrold, M. F. *Nature* **1994**, *367*, 718.

(17) Clemmer, D. E.; Shelimov, K. B.; Jarrold, M. F. *J. Am. Chem. Soc.* **1994**, *116*, 5971.

(18) Shelimov, K. B.; Clemmer, D. E.; Jarrold, M. F. *J. Phys. Chem.* **1994**, *98*, 12819.

(19) Shelimov, K. B.; Clemmer, D. E.; Jarrold, M. F. *J. Phys. Chem.* **1995**, *99*, 11376.

(20) Clemmer, D. E.; Hunter, J. M.; Shelimov, K. B.; Jarrold, M. F. *Nature* **1994**, *372*, 248. Clemmer, D. E.; Jarrold, M. F. *J. Am. Chem. Soc.* In press.

0002-7863/96/1518-1139$12.00/0

recently. These studies show that C_n^+ and MC_n^+ clusters have the same basic structural isomers. These include planar mono-, bi-, and polycyclic C_n^+ and MC_n^+ rings, graphite sheets, and fullerenes (linear chains are also observed for small C_n^+ clusters). For both C_n^+ and MC_n^+ clusters, monocyclic rings are the only isomer observed for $n = 10-20$. Bicyclic rings are the dominant isomer around $n = 30$, and polycyclic rings become important for larger clusters. For MC_n^+ clusters, fullerenes and graphite sheets start to dominate at substantially smaller cluster sizes than for pure carbon clusters. For C_n^+ clusters, fullerenes become the dominant isomer around $n = 50$ and graphite sheets are at best a minor isomer for all clusters studied. For MC_n^+ clusters, graphite sheets are the dominant isomer around $n = 32$ and fullerenes dominate for $n > 35$. Ion mobility studies can also reveal information about the location of the metal atom in metallofullerenes. Small ($n \leq 35$) MC_n^+ metallofullerenes are non-endohedral; LaC_n^+ ($n > 37$) and NbC_{2n}^+ ($2n \geq 36$) fullerenes are endohedral, while the metal atom seems to occupy a position in the carbon network for NbC_{2n+1}^+ fullerenes. Annealing studies of C_n^+ and MC_n^+ clusters have provided important insight into the fullerene formation mechanism. Both pure[21,22] and metal-containing[16,18] carbon rings isomerize into fullerenes when collisionally heated. The efficiency of this process is much higher for MC_n^+ clusters than for C_n^+ clusters.[16,18]

In the present paper we report gas phase ion mobility studies of the structures and isomerization of $La_2C_n^+$ ($n = 1-100$) clusters. We find that along with the structures similar to those observed for C_n^+ and MC_n^+ clusters (monocyclic rings, graphite sheets, and fullerenes), new classes of structures are formed for $La_2C_n^+$ clusters. These appear to be three-dimensional complexes of metal-containing carbon clusters. For example, a fusion of two planar metal-containing carbon rings can produce a stable three-dimensional ring complex. Structures of this type are formed instead of planar rings for $La_2C_n^+$ ($n \geq 17$) clusters. Isomers which appear to be complexes of metallofullerenes and metal-containing rings are abundant for large ($n \geq 50$) $La_2C_n^+$ clusters. Thus it seems that the metal atoms are able to act as nucleation centers for the formation of multimetal-containing carbon clusters.

Experimental Section

The experimental apparatus used in this study has been described in detail previously.[23,24] Briefly, La-containing carbon cluster cations are generated by laser vaporization of a composite LaC_2/graphite rod. The rods were prepared by mixing LaC_2 (Johnson Matthey, 99%) and graphite powder (Johnson Matthey, 99.9995%) in a 1:60 La:C ratio and subsequently pressing the mixture into cylindrical pellets. Short (50 μs) pulses of mass-selected cluster cations are accelerated to 50−350 eV and focused into the drift tube containing He buffer gas at a pressure around 5 Torr. Upon entering the drift tube, clusters are rapidly heated through collisions with buffer gas atoms, and if the injection energy is high enough they may isomerize or fragment. The clusters then travel slowly across the drift tube under the influence of a weak (13.12 V/cm) electric field. The drift time depends on the physical size of the cluster, so that isomers with different shapes are separated in the drift tube. Upon exiting the drift tube, the clusters are mass-analyzed, detected with an off-axis collision dynode and dual microchannel plates, and their arrival times at the detector are recorded with a multichannel analyzer. The drift time distributions obtained in this way provide information about the number of isomers present, their relative abundances, and their mobilities in the helium buffer gas. Reduced mobilities were obtained from the expression

$$K_o = \frac{L}{t_D E} \frac{P}{760} \frac{273.2}{T}$$

where L is the length of the drift tube, t_D is the drift time, E is the electric field, P is the pressure of the buffer gas in Torr, and T is the buffer gas temperature in K. Information about the shapes of individual isomers can be deduced from their reduced mobilities, as discussed in detail below.

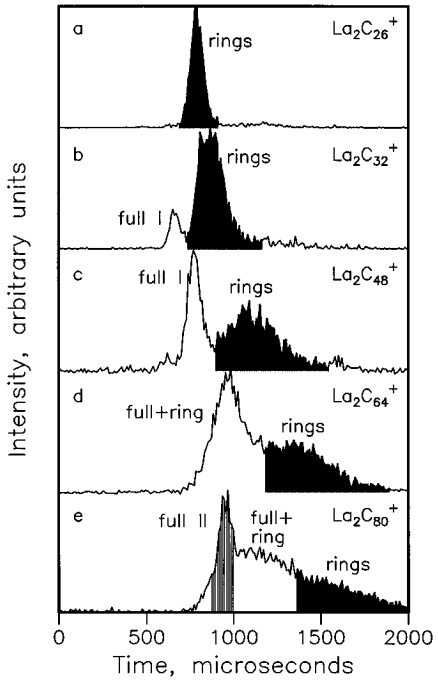

Figure 1. Drift time distributions of some $La_2C_n^+$ clusters recorded at low (50 eV) injection energy. The isomers observed are metal-containing carbon rings (labeled "rings"), two metallofullerene isomers (labeled "full I" and "full II"), and fullerene-ring complexes (labeled "full+ring").

Results

1. Isomer Distributions. Figure 1 shows the drift time distributions for $La_2C_{26}^+$, $La_2C_{32}^+$, $La_2C_{48}^+$, $La_2C_{64}^+$, and $La_2C_{80}^+$ recorded at low (50 eV) injection energy. These distributions represent the isomer populations for clusters coming directly from the source (there is essentially no collision-induced isomerization or dissociation at this injection energy). The drift time distribution for $La_2C_{26}^+$ is typical of $La_2C_n^+$ clusters with $n < 28$. For all clusters from La_2^+ to $La_2C_{27}^+$ (except $La_2C_{10}^+$ as noted below) only one peak is observed in the drift time distributions. As discussed in detail below, we attribute this peak to two- and three-dimensional complexes of metal-containing carbon rings and therefore we will refer to it as the *rings* peak. Figure 2 shows the fwhms (full widths at half-maximum) of the *rings* peak as a function of the cluster size. The fwhms are normalized to account for their systematic increase with the cluster size (due to the increase in the drift time). This normalization is performed by dividing the measured fwhm by the fwhm calculated using the gas phase ion transport equation,[25] assuming the presence of only one structural isomer. An abrupt increase in the width of the *rings* peak observed for $La_2C_8^+$, $La_2C_9^+$, and $La_2C_{10}^+$ indicates that at least two different structural isomers exist for these three clusters. Under improved resolution conditions (25 μs ion

(21) Hunter, J. M.; Fye, J. L.; Jarrold, M. F. *Science* **1993**, *260*, 784. von Helden, G.; Gotts, N. G.; Bowers, M. T. *Nature* **1993**, *363*, 6424.
(22) Hunter, J. M.; Fye, J. L.; Roskamp, E. J.; Jarrold, M. F. *J. Phys. Chem.* **1994**, *98*, 1810.
(23) Jarrold, M. F.; Bower, J. E.; Creegan, K. *J. Chem. Phys.* **1989**, *90*, 3615. Jarrold, M. F.; Bower, J. E. *J. Chem. Phys.* **1992**, *96*, 9180.
(24) Hunter, J. M.; Fye, J. L.; Jarrold, M. F. *J. Chem. Phys.* **1993**, *99*, 1785.
(25) McDaniel, E. W.; Mason, E. A. *Transport Properties of Ions in Gases*; Wiley: New York, 1988.

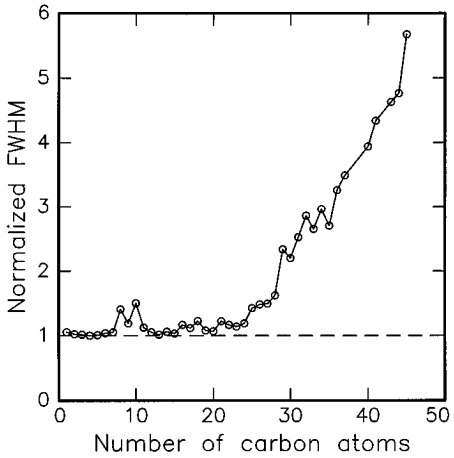

Figure 2. The full widths at half-maximum (fwhms) of the *ring* peak in the drift time distributions as a function of the cluster size. The fwhms are normalized in order to account for their systematic increase with the drift time.

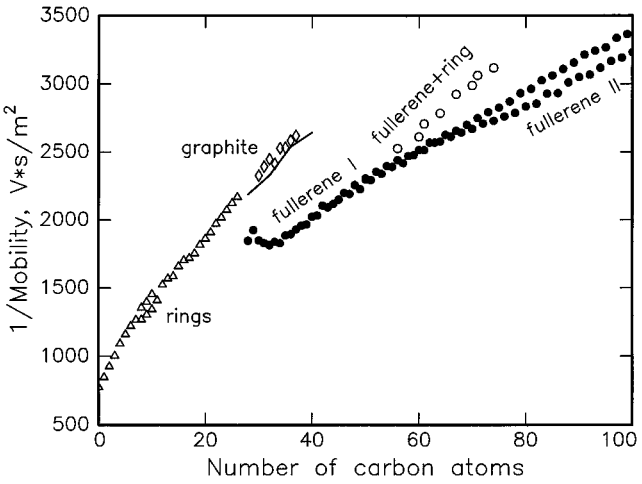

Figure 3. Plot of the inverse mobilities of $La_2C_n^+$ isomers against the cluster size. The solid line shows the calculated mobilities of $La_2C_n^+$ graphite sheets (see text).

pulses), two peaks can actually be resolved in the drift time distribution for $La_2C_{10}^+$. For $La_2C_n^+$ ($n = 11-15$) clusters, the width of the *rings* peak in the drift time distributions is close to that expected for just one structural isomer, while for clusters with 16−24 carbon atoms it is slightly (by around 1.2) broader. However, starting at $La_2C_{25}^+$ the width of the peak increases significantly with cluster size (see Figure 1b−e and Figure 2), indicating that multiple *ring* isomers are present for large $La_2C_n^+$ clusters. A detailed analysis of the geometries of the individual isomers contributing to this broad peak is impossible, so for large $La_2C_n^+$ clusters we can no longer be sure that these isomers are metal-containing carbon rings. However, for brevity we will still refer to the broad peak at long drift times in the unannealed drift time distributions of large $La_2C_n^+$ clusters as *rings*. *Rings* comprise at least 50% of the isomer distribution for unannealed clusters up to around $La_2C_{56}^+$ (see Figure 1b,c) and remain abundant for larger clusters.

A second peak appears in the drift time distributions of $La_2C_n^+$ clusters at $La_2C_{28}^+$. The isomer corresponding to this peak is more compact (has a smaller drift time) than the *rings* (see Figure 1b). The normalized fwhm of this second peak is close to one for clusters up to around $La_2C_{45}^+$ (see Figure 1c), implying that just one isomer, or a group of similarly shaped isomers, accounts for this peak in this size range. Below we will refer to this isomer as *fullerene I*. The relative abundance of *fullerene I* increases with cluster size to reach 30−35% of the unannealed isomer distribution around $La_2C_{45}^+$. For $n \geq 36$, $La_2C_n^+$ *fullerene I* is more abundant for clusters with an odd number of carbon atoms. For clusters larger than $La_2C_{45}^+$ the width of the second peak in the drift time distributions starts to increase (see Figure 1c,d), and the center of the peak shifts to longer drift times than those expected for *fullerene I*. Apparently multiple isomers contribute to this peak for large $La_2C_n^+$ clusters, and it seems that these isomers are different from *fullerene I*. We will refer to these isomers as *fullerenes+rings*. The relative abundance of *fullerenes+rings* increases with cluster size for clusters up to $La_2C_{64}^+$ to reach around 50%, and then remains close to this value for clusters up to $La_2C_{80}^+$. For larger $La_2C_n^+$ clusters the broad *ring* and *fullerene+ring* peaks can no longer be clearly distinguished (Figure 1e).

Around $La_2C_{72}^+$ a new peak with a smaller drift time than the *fullerenes + rings* becomes apparent for clusters with an even number of carbon atoms (see Figure 1e). This peak will be referred to as *fullerene II*. No *fullerene II* feature is observed for $La_2C_n^+$ clusters with an odd number of carbon atoms. Unlike the *rings* and the *fullerene I − fullerenes+rings* peaks, the *fullerene II* peak does not become broader with increasing cluster size. The relative abundance of *fullerene II* systematically increases with cluster size and reaches around 30−35% for unannealed $La_2C_{100}^+$.

Figure 3 shows the mobilities of the $La_2C_n^+$ isomers mentioned above, plotted against cluster size. The mobilities of the two unresolved isomers of $La_2C_8^+$, $La_2C_9^+$, and $La_2C_{10}^+$ were determined by fitting peaks calculated using the gas phase ion transport equation[25] to peaks in the drift time distributions. No mobility data for *rings* larger than $La_2C_{26}^+$ are shown since for these larger clusters the *rings* peak in the drift time distributions is wide and does not represent a single structure. The mobilities of *fullerenes I* and *fullerenes II* shown in Figure 3 were measured at high injection energies, as discussed below. The mobilities of *fullerenes+rings* shown in the figure correspond to the center of the broad *fullerene+ring* distribution. Mobilities of *fullerenes+rings* are shown for only a few clusters to illustrate their deviation from *fullerene I* mobilities. Justification of our structural assignments and a detailed discussion of the possible structures of the observed families of isomers are given below.

Figure 4 compares the unannealed drift time distributions for C_n^+, LaC_n^+, and $La_2C_n^+$ ($n = 26$ and 60) clusters. This comparison shows that isomer distributions observed for $La_2C_n^+$ clusters are substantially different from those observed for C_n^+ [15] and LaC_n^+ [19] clusters. Multiple isomers are observed in the drift time distributions for both C_n^+ and LaC_n^+ in the $n = 20-40$ size range. For example, two isomers (mono- and bicyclic rings) are present in the drift time distribution for C_{26}^+ (see Figure 4a) and three isomers (two ring isomers and a graphite sheet) are observed for LaC_{26}^+ (see Figure 4b), while we observe only one peak in the drift time distribution for $La_2C_{26}^+$ (see Figure 4c). Isomer distributions for large ($n \geq 40-50$) C_n^+ and LaC_n^+ clusters are dominated by narrow fullerene peaks (see Figure 4d,e), while the broad *fullerenes+rings* feature dominates the drift time distributions for $La_2C_n^+$ ($45 \leq n \leq 80$) clusters (and larger clusters with an odd number of carbon atoms) (see Figure 4f). This suggests that the presence of the second metal atom substantially changes the cluster growth mechanism.

2. Collisional Annealing and Isomer Interconversion. When the injection energy is increased, collisonal heating may lead to annealing of the isomer distribution. The observed annealing processes are illustrated in Figure 5 for several selected $La_2C_n^+$ clusters. For clusters smaller than $La_2C_{28}^+$ there is essentially no change in the drift time distributions with

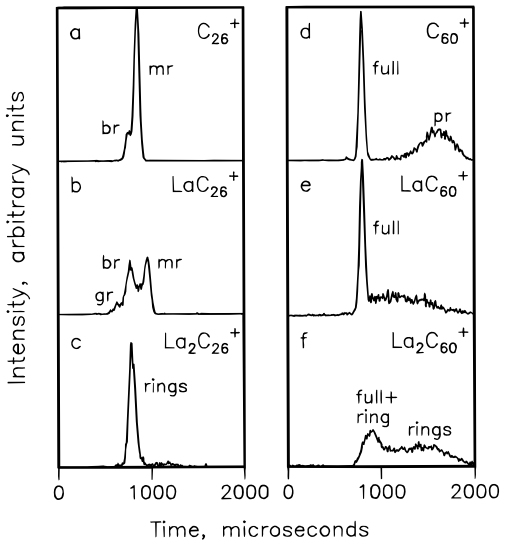

Figure 4. Normalized drift time distributions of C_n^+, LaC_n^+, and $La_2C_n^+$ (n = 26 and 60) clusters recorded at 50 eV injection energy. The C_n^+ and LaC_n^+ isomers seen in these distributions are mono-, bi-, and polycyclic rings (labeled "mr", "br", and "pr", respectively), graphite sheets (labeled "gr"), and fullerenes (labeled "full"). The $La_2C_n^+$ isomer labeling is the same as in Figure 1.

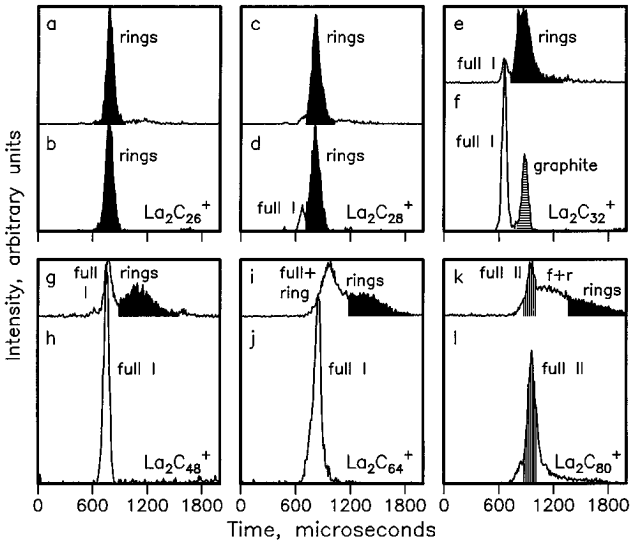

Figure 5. Normalized drift time distributions of several $La_2C_n^+$ clusters recorded at low and high injection energies. The injection energies were the following: 50 eV (a, c, e, g, i, k), 200 eV (d), 250 eV (b, f), and 300 eV (h, j, l). The isomer labeling is the same as in Figure 1 ("f+r" stands for *fullerene+ring*). Shoulders at smaller drift times on the fullerene peaks in Figure 5j,l are due to contaminants.

increasing injection energy (see Figure 5a,b), i.e. small $La_2C_n^+$ *rings* do not isomerize into other structures. Moreover, the *rings* peak in the drift time distributions of $La_2C_n^+$ (n < 30) clusters does not become narrower as the injection energy is increased (see Figure 5a−d), suggesting that various *ring* isomers have similar stabilities or do not interconvert. Larger ($n \geq 30$) *rings* undergo significant structural changes upon collisional heating (see Figure 5e−h). The amount of fragmentation observed for $La_2C_{32}^+$ and $La_2C_{48}^+$ at high (250−350 eV) injection energies does not exceed 10%, so that the changes observed in the drift time distributions with increasing injection energy are due primarily to isomerization processes. For $La_2C_{48}^+$, essentially all collisionally excited *rings* isomerize into *fullerene I*. *Fullerene I* is also the major product of $La_2C_{32}^+$ *rings* isomerization. However, for $La_2C_{32}^+$ at an injection energy of 250 eV, an intense narrow feature (labeled *graphite* in Figure 5f) is still left in place of the original broad *ring* peak. Further

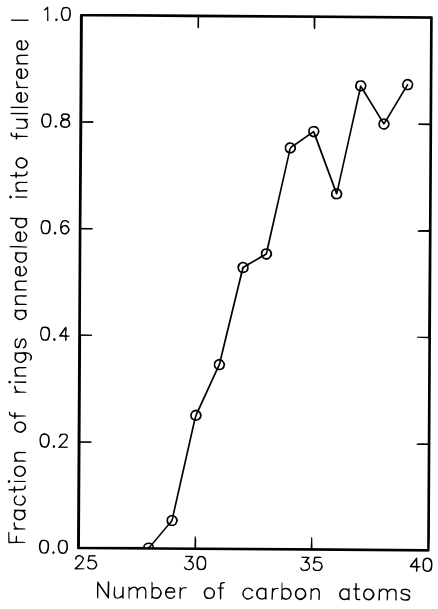

Figure 6. The fraction of $La_2C_n^+$ *rings* annealed into *fullerene I* at an injection energy of 250 eV as a function of the cluster size.

increase of the injection energy does not lead to annealing of the remaining isomer into *fullerene I*, but rather to its dissociation. It therefore seems unlikely that the *graphite* peak represents a structure that is similar to $La_2C_{32}^+$ *rings*, although it has a similar drift time. It is more likely that this peak corresponds to a different structure, which itself is at least partially a product of the annealing of the original *ring* distribution. The fact that the annealing of the broad *ring* distribution for smaller clusters ($La_2C_{26}^+$ to $La_2C_{29}^+$) does not result in the formation of a narrower isomer distribution also speaks in favor of this interpretation. The inverse mobilities of the *graphite* isomer are plotted in Figure 3. This isomer can be clearly seen in the high injection energy drift time distributions only over a narrow cluster size range (from $La_2C_{30}^+$ to $La_2C_{37}^+$), where it presumably can compete with *fullerene I* as an isomerization product of the *rings*. For larger $La_2C_n^+$ clusters, the isomerization of *rings* into *fullerene I* becomes dominant, so that only the *fullerene I* peak is observed in drift time distributions at high injection energies (see Figure 5h).

The competition between the pathways for the transformation of collisionally excited $La_2C_n^+$ (n = 25−40) *rings*—isomerization into *fullerene I*, isomerization into *graphite*, and dissociation—is illustrated in Figure 6. This figure shows the fraction of *rings* annealed into *fullerene I* as a function of cluster size. In the low injection energy drift time distributions the *graphite* peak is buried under the broad *ring* distribution, and no attempt has been made to estimate what fraction of this distribution it accounts for. Therefore the relative abundance of *rings* in the unannealed cluster beam is overestimated, and the data presented in Figure 6 show a lower limit to the fraction of *rings* annealed into *fullerene I*. For clusters smaller than $La_2C_{28}^+$ no isomerization of *rings* into *fullerene I* is observed. It is possible that a certain fraction of *rings* for $La_2C_{26}^+$ to $La_2C_{29}^+$ isomerizes to form *graphite*, but this isomerization process cannot be followed because the narrow *graphite* peak is buried under the broad *ring* distribution even at high injection energies. Most of the $La_2C_n^+$ (n < 29) *rings* dissociate as the injection energy is increased further. For larger clusters the fraction of *rings* that dissociates at high injection energies goes down, while the fraction that isomerizes into *fullerene I* and *graphite* increases. For clusters between $La_2C_{31}^+$ and $La_2C_{37}^+$ the fraction of *rings* annealed into *fullerene I* is determined primarily by the competition between isomerization into *graphite* and *fullerene I*. For clusters

Table 1. Estimated Activation Energies for the Isomerization of Pure and Metal-Containing Carbon Rings into Fullerenes

cluster	activation energy, eV
$La_2C_{33}^+$	2.3
$La_2C_{34}^+$	2.1
$La_2C_{43}^+$	1.9
LaC_{35}^+	3.1[a]
LaC_{36}^+	3.1[a]
C_{40}^+	2.8[b]

[a] Reference 19. [b] Reference 22.

larger than $La_2C_{37}^+$ essentially all the original isomer distribution is converted into *fullerene I*.

For $La_2C_{33}^+$, $La_2C_{34}^+$, and $La_2C_{43}^+$ we have measured the relative abundance of *fullerene I* as a function of the injection energy over a 50−180 eV range. The annealing thresholds obtained in this way can be used to estimate the activation energies for isomerization of *rings* into *fullerene I*, as discussed in detail elsewhere.[26] The fraction of the ions' kinetic energy transferred into the internal energy by collisions with buffer gas atoms is estimated using a modified impulsive collision model[19,26,27] and the isomerization rate of a vibrationally excited cluster is calculated using RRK theory.[28] The reaction time is assumed to be of the order of the time between collisions with buffer gas atoms. Although activation energy estimates obtained using this model are not expected to be accurate to more than 0.5 eV, the relative values are believed to be more reliable. The estimated activation energies for isomerization of *rings* into *fullerenes* are listed in Table 1. The table shows that the activation energies for isomerization of $La_2C_n^+$ *rings* are significantly smaller than those for isomerization of C_n^+ and LaC_n^+ rings.

For clusters larger than $La_2C_{50}^+$, *fullerenes*+*rings* comprise a significant fraction of the drift time distributions at low injection energies, while *fullerene I* is not resolved as a separate peak (see Figure 1d,e). When collisionally heated, *fullerenes*+*rings* (along with *rings*) readily transform into a single relatively narrow feature (see Figure 5i−l). The amount of fragmentation for $La_2C_{64}^+$ and $La_2C_{80}^+$ at 300 eV is less than 12%, so that the isomerization processes are the primary source of the observed transformations. The feature observed at high injection energies is narrow enough to be accounted for by just one isomer for all $La_2C_n^+$ ($n < 64$) clusters and $La_2C_n^+$ ($n > 64$) clusters with an odd number of carbon atoms, but broader for $La_2C_n^+$ ($n \geq 64$) clusters with an even number of carbon atoms (see Figure 5l). The mobilities corresponding to this feature are plotted as filled circles in Figure 3. For clusters smaller than $La_2C_{64}^+$, and larger clusters with an odd number of carbon atoms, the mobilities clearly correlate to those of small *fullerenes I*, suggesting a similar structure. For $La_2C_{2n}^+$ ($2n \geq 80$) clusters, the mobilities measured at 300 eV are essentially the same as those measured for *fullerene II* at 50 eV, so that *fullerene II* is the major annealing product. Finally, for $La_2C_{2n}^+$ ($64 \leq 2n < 80$) clusters the measured mobilities lie in between those expected for *fullerene I* and *fullerene II*, suggesting the coexistence of both isomers.

3. Collision-Induced Dissociation of $La_2C_n^+$ Clusters. In addition to isomerizing, collisionally excited $La_2C_n^+$ clusters dissociate. Because of the small $La_2C_n^+$ ion signal we were only able to perform detailed dissociation studies for clusters with up to 40 carbon atoms. The main pathways for the dissociation of $La_2C_n^+$ ($n \leq 30$) clusters (where *rings* are the major isomer) include the loss of LaC_4^+ (and small amounts of other LaC_{2n}^+ ($n = 1-4$) fragments), the loss of C_3 (and small amounts of C_5), and the loss of C_{4n+2} ($n = 2-5$) fragments. The branching ratios for these three dissociation pathways, as a function of cluster size, are plotted in Figure 7. The loss of LaC_4^+ and other LaC_{2n}^+ fragments is the major dissociation pathway for clusters up to $La_2C_{21}^+$. Small clusters with an odd number of carbon atoms ($La_2C_7^+$ to $La_2C_{13}^+$) also lose significant amounts of C_3, while the loss of C_3 is less important for their even-numbered neighbors. The magnitude of this odd−even variation decreases in the $La_2C_{11}^+$ to $La_2C_{20}^+$ size range. Loss of LaC_4^+ and other small LaC_{2n}^+ fragments is the main dissociation channel for LaC_n^+ rings,[19] while the loss of C_3 and C_5 dominates for pure C_n^+ ($n \leq 30$) rings.[29] The dissociation patterns of small $La_2C_n^+$ clusters (Figure 7) show a strong tendency to form La-containing fragments with an even number of carbon atoms. This presumably reflects higher thermodynamic stability of these species compared to their odd-numbered counterparts. For larger $La_2C_n^+$ clusters the odd−even variation in dissociation patterns becomes less pronounced, suggesting that the difference in the thermodynamic stabilities of even- and odd-numbered clusters is reduced. For $La_2C_{22}^+$ and larger *rings* the loss of C_{4n+2} fragments is the dominant dissociation pathway. The loss of C_{4n+2} fragments (which are presumably aromatic rings) has been observed as the major fragmentation channel for large ($n > 30$) C_n^+ clusters[30,31] and for LaC_n^+ clusters with an even number of carbon atoms (where C_{4n+2} fragments are complementary to LaC_4^+ and other LaC_{2m}^+ fragments).[19]

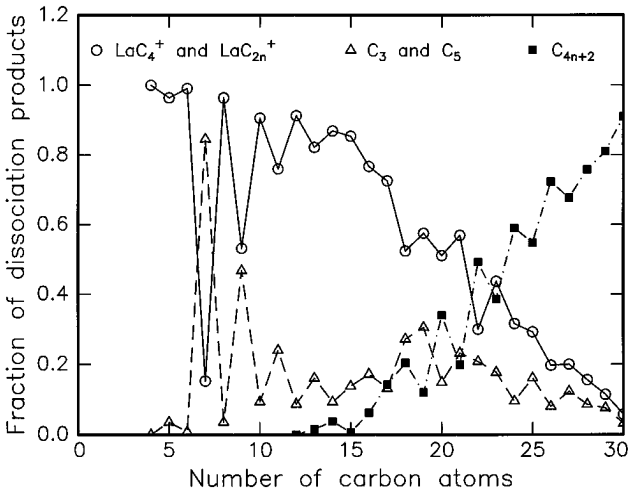

Figure 7. The branching ratios between the dissocaition pathways of $La_2C_n^+$ *rings* as a function of the cluster size. The three dissociation pathways include the loss of LaC_4^+ (and smaller amounts of other LaC_{2n}^+, $n = 1-4$, fragments), the loss of C_3 (and a smaller amount of C_5), and the loss of C_{4n+2} ($n = 2-5$) fragments.

For several small $La_2C_n^+$ clusters we have performed detailed measurements of the amount of fragmentation as a function of the injection energy. Dissociation thresholds can then be estimated in a fashion similar to that described above for the isomerization threshold calculations. The dissociation thresholds estimated for $La_2C_n^+$ *rings* are very close to those measured for C_n^+ rings and larger than those determined for LaC_n^+ rings (see Table 2). Thus the addition of a single metal atom to a carbon ring destabilizes the planar ring geometry, while the addition of a second La atom presumably causes a transforma-

(26) Jarrold, M. F.; Honea, E. C. *J. Phys. Chem.* **1991**, *95*, 9181.
(27) Uggerud, E.; Derrick, P. J. *J. Phys. Chem.* **1991**, *95*, 1430.
(28) Steinfeld, J. I.; Francisco, J. S.; Hase, W. L. *Chemical Kinetics and Dynamics*; Prentice-Hall: Englewood Cliffs, NJ, 1989.
(29) Geusic, M. E.; Jarrold, M. F.; McIlrath, T. J.; Bloomfield, L. A.; Freeman, R. R.; Brown, W. L. *J. Chem. Phys.* **1987**, *86*, 3862.
(30) Radi, P. P.; Bunn, T. L.; Kemper, P. R.; Molchan, M. E.; Bowers, M. T. *J. Chem. Phys.* **1988**, *88*, 2809.
(31) Shelimov, K. B.; Hunter, J. M.; Jarrold, M. F. *Int. J. Mass Spectrom. Ion Proc.* **1994**, *138*, 17.

Table 2. Estimated Dissociation Thresholds for Pure and La-Containing Carbon Rings (eV)

n	C_n^+ [a]	LaC_n^+	$La_2C_n^+$
19	5.2	4.6	5.2
20	5.2	4.5	5.0
25	4.7	4.4	5.0
26	4.8	3.9	4.8

[a] Reference 31.

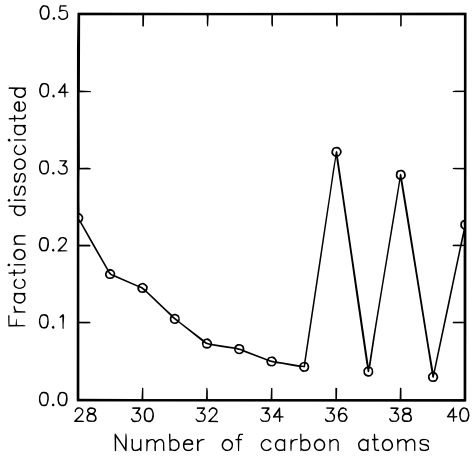

Figure 8. The fraction of $La_2C_n^+$ clusters dissociated at the injection energy of 250 eV as a function of cluster size. The major fragmentation channel is the loss of La^+ (and a smaller amount of LaC_2^+) for $La_2C_{36}^+$, $La_2C_{38}^+$, and $La_2C_{40}^+$ and the loss of C_{4n+2} ($n = 3-5$) fragments for other clusters.

tion to a geometry, which is more stable toward dissociation. The results of the mobility measurements discussed above lead to a similar conclusion. We have also recorded drift time distributions for the dissociation products resulting from the loss of C_3 fragments from several $La_2C_n^+$ *rings* ($n = 20$, 23, 26, 29) and the loss of C_{18} from $La_2C_{28}^+$. These drift time distributions are similar to those for clusters of the same size coming directly from the source (one peak for $La_2C_n^+$ ($n = 17$, 20, 23, 26) and two peaks for $La_2C_{10}^+$). The mobilities measured for the dissociation products are within 1.5% of those for the *rings* formed in the source. Thus $La_2C_n^+$ *rings* seem to have the same structures regardless of whether they are formed through the association of smaller fragments or through the dissociation of larger clusters.

With the appearance of *fullerene I* and *graphite* the dissociation pattern of $La_2C_n^+$ clusters changes dramatically. The main dissociation pathway for clusters between $La_2C_{36}^+$ and $La_2C_{64}^+$ is the loss of La^+ (and smaller amounts of LaC_2^+ and LaC_4^+). The change in the dissociation pattern is accompanied by a sharp increase in the amount of fragmentation for clusters with an even number of carbon atoms, as illustrated in Figure 8. Since loss of La^+ is not observed for $La_2C_n^+$ *rings*, it must be due to the dissociation of *fullerene I*, which is the major annealing product of the *rings* in this size range. The *fullerene I* isomer for $La_2C_n^+$ ($n = 36$, 38, 40) clusters comprises only around 20% of the unannealed isomer distribution and around 90% of isomer distribution at an injection energy of 250 eV. Thus the observed 25−30% *fullerene I* fragmentation (see Figure 8) must be due primarily to the dissociation of *fullerenes I* formed as the result of the isomerization of *rings*. This dissociation is probably driven by the exothermicity of the isomerization process. The loss of La^+ from $La_2C_n^+$ ($n = 36-64$) clusters with an even number of carbon atoms is a signature of metallofullerene formation and in this respect is analogous to the loss of C_2 units from C_n^+ fullerenes formed through the isomerization of bi- and polycyclic pure carbon rings.[22]

Discussion

1. Structural Assignments. (a) The Fullerene Families. From the comparison with the previously measured mobilities of C_n^+ and LaC_n^+ [18] fullerenes we assign the *fullerene I* and *II* families of $La_2C_n^+$ isomers to metallofullerene structures, as discussed in detail in a separate publication.[32] When a metal atom moves from a non-endohedral position to an endohedral position the mobility of a metallofullerene increases by 5−10%.[18,20] Mobility variations of this magnitude observed for $La_2C_n^+$ fullerenes (see Figure 3) indicate that the *fullerene I* isomers have two non-endohedral metal atoms for $n = 28-29$ and one endohedral and one non-endohedral metal atom for $n = 31-100$ ($La(La@C_n)^+$ or $La@C_nLa^+$ structure), while both metal atoms are endohedral for the *fullerene II* isomers (the $La_2@C_n^+$ structure). For $La_2C_{2n}^+$ ($2n \geq 64$) clusters, fullerenes with two and one endohedral metal atoms coexist, but are not resolved at room temperature, giving rise to broader peaks in the drift time distributions (see Figure 5l). The two structures can be resolved at lower buffer gas temperatures.[32]

The fact that $La_2C_n^+$ ($36 \leq n \leq 63$) fullerenes with an odd number of carbon atoms are more abundant than the even-numbered ones in the unannealed cluster beam suggests that they are stabilized by the non-endohedral La atom occupying the defect site in the C_{n+1} cage (the $La@C_nLa^+$ structure). A similar networked structure has been proposed for small LaC_{2n+1}^+ and all NbC_{2n+1}^+ metallofullerenes.[18,20] The fact that, unlike pure C_n^+ fullerenes, dilanthanum metallofullerenes with 28 and 29 carbon atoms are easily observable in our experiments suggests that the strain energy of these small $La_2C_n^+$ fullerenes is substantially reduced, i.e. $La_2C_{28}^+$ and $La_2C_{29}^+$ fullerenes are also networked. Figure 3 shows that in the $2n = 40-62$ size range the mobilities of $La_2C_{2n}^+$ fullerenes are slightly (by about 0.5%) smaller than the mobilities of $La_2C_{2n+1}^+$ fullerenes. If the $La_2C_{2n}^+$ fullerenes were also networked, the fullerene mobilities would be expected to decrease steadily with cluster size. Thus it is likely that the non-endohedral metal atom in $La_2C_{2n}^+$ ($2n \geq 40$) fullerenes resides outside the carbon cage (the $La(La@C_n)^+$ structure).

The metallofullerene structure with one endohedral metal atom proposed for $La_2C_n^+$ ($n \geq 31$) clusters is consistent with the fragmentation behavior illustrated in Figure 8. Studies of the LaC_n^+ system have shown that LaC_{36}^+ is the smallest stable endohedral La-containing metallofullerene.[18,33] Thus the enhanced loss of La^+ from $La_2C_{36}^+$ and larger $La_2C_{2n}^+$ clusters (see Figure 8) must be due to the formation of stable $La@C_{2n}^+$ metallofullerenes upon the collisional heating of the original $La_2C_{2n}^+$ isomer distribution. The fact that the loss of La^+ is *not* observed for $La_2C_{32}^+$ and $La_2C_{34}^+$ suggests that in these smaller metallofullerenes the non-endohedral metal atom is a part of the fullerene cage. Apparently, the incorporation of metal atoms into small fullerene cages with an even number of carbon atoms makes these cages larger so that they can more easily accommodate the endohedral metal atom.

(b) The Graphite Family. For LaC_n^+ clusters the isomer assigned to roughly planar metal-containing graphite sheets exists over a wide range of sizes.[18] The mobilities of LaC_n^+ graphite sheets are by 9−14% smaller than the mobilities of pure C_n^+ graphite sheets. This difference can be accounted for by the La atom coordinated to dangling bonds on the edge of a graphite sheet. The solid line in Figure 3 shows the results of the mobility estimates for planar roughly circular C_n graphite sheets with two La atoms attached to the edge. Cluster mobility estimates reported in the present work have been performed

(32) Shelimov, K. B.; Jarrold, M. F. *J. Am. Chem. Soc.* **1995**, *117*, 6404.
(33) Guo, T.; Smalley, R. E.; Scuseria, G. E. *J. Chem. Phys.* **1993**, *99*, 352.

using the expression[25]

$$K_o = \frac{(18\pi)^{1/2}}{16}\left[\frac{1}{m_I}+\frac{1}{m_B}\right]^{1/2}\frac{e}{(k_B T)^{1/2}}\frac{1}{\sigma}\frac{1}{N}$$

where m_I and m_B are the masses of the cluster ion and the buffer gas atom respectively, N is the buffer gas number density, and σ is the average collision cross section. The collision cross section is calculated by averaging over all possible orientations of the cluster in space, assuming hard-sphere interactions. In order to estimate the collision cross section, one needs to know the geometry of the cluster and two empirical parameters—the hard-sphere distances for C−He and La−He collisions. The geometries of the pure carbon graphite sheets were optimized in quantum chemical calculations at the MNDO level, and the La−C bond distances and bond angles were determined in *ab initio* calculations for small model systems.[19] The *ab initio* calculations were performed at the Hartree−Fock level with basis sets of double-ζ quality and an 11-electron relativistic effective core potential on La,[34] using the Gaussian-92 program.[35] The hard-sphere distance for C−He collisions (2.7 Å) was determined by fitting the mobility data for pure carbon clusters. The La−C hard-sphere collision distance is taken to be 3.07 Å, as determined from the measured mobilities of La^+ and La_2^+.

The mobilities of the graphite sheets with two metal atoms attached to the edges (the solid line in Figure 3) are in fairly good agreement with the mobilities of $La_2C_n^+$ isomers from the *graphite* family. Both LaC_n^+ graphite sheets and $La_2C_n^+$ *graphite* isomers seem to be the products of the isomerization of metal-containing carbon rings and are most abundant for clusters with 30−34 carbon atoms. For these reasons we assign the *graphite* family of $La_2C_n^+$ isomers to metal-containing graphite sheets. This assignment refers to a general class of structures rather than to a specific cluster geometry. For example, we cannot rule out the possibility that some pentagonal defects may be present in the carbon network forming the graphite sheet. However, the large (17−19%) difference between the mobilities of pure C_n^+ and $La_2C_n^+$ graphite sheets suggests that the metal atoms must be in a position where they are exposed to the collisions with buffer gas atoms to the largest extent. Hence the position of the metal atoms on the edge of a graphite sheet seems to be the most plausible.

(c) The Ring Family. The mobilities of $La_2C_n^+$ *rings* change with cluster size in a non-uniform way. Figure 3 shows that the inverse mobilities of the *rings* increase roughly linearly with cluster size in the $n = 1-6$ and 17−26 ranges. A linear increase in the inverse mobility with cluster size is typical of one- and two-dimensional growth patterns when a single structural isomer is present. Clearly, the growth patterns of $La_2C_n^+$ *rings* in the $n = 1-6$ and 17−26 size ranges are different, and they will be analyzed separately below.

It has been established that small C_n^+ clusters can be either linear chains (for $n = 3-10$) or planar rings (for $n > 6$),[15,36] while small LaC_n^+ ($n > 2$) clusters are rings.[19] These two structures were considered as the candidates for $La_2C_n^+$ ($n < 10$) *rings*. The solid line in Figure 9 shows the calculated mobilities of planar $La_2C_n^+$ rings with both metal atoms inserted into the ring (as in structure **A** in Figure 9). The ring geometries have been optimized in quantum chemical calculations at the Hartree−Fock level as described above. The calculated mobilities are in excellent agreement with the experiment for $n = 3-6$. On the other hand, the calculated mobilities of linear $La_2C_n^+$ ($n > 0$) chains (plotted as the dash-dotted line in Figure 9) are too small to account for the experimental results. Thus small $La_2C_n^+$ ($n > 0$) clusters appear to be planar rings (or bent chains for $n = 1, 2$). In their ion mobility studies, von Helden *et al*. reached a similar conclusion about the structures of small $Fe_2C_n^-$ clusters.[37]

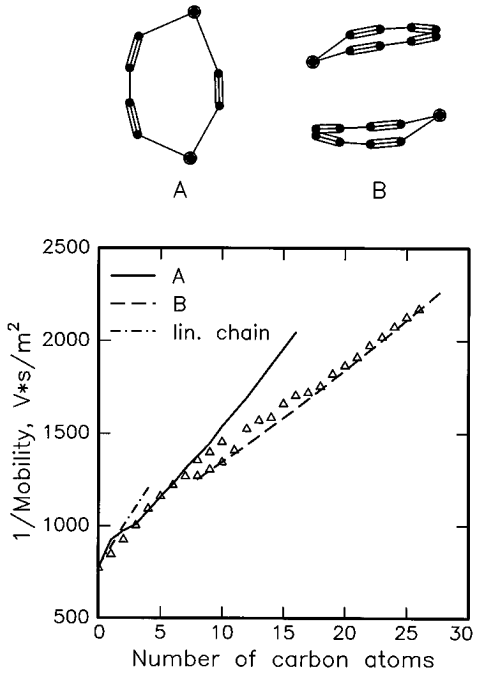

Figure 9. The proposed structures of planar (**A**) and three-dimensional (**B**) $La_2C_n^+$ *rings*. The points on the plot show the measured mobilities of $La_2C_n^+$ *rings* and the lines show the mobilities calculated for structures **A** and **B** and for linear La-terminated carbon chains (see text).

We have performed Hartree−Fock geometry optimizations for several plausible $La_2C_n^+$ ($n = 1-6$) ring structures with the metal atoms in various positions with respect to each other and to the ring. Structures with two La atoms inserted into the ring and separated from each other by carbon atoms (such as the $La_2C_6^+$ ring shown as structure **A** in Figure 9) were found to be the lowest energy ring structure for all cluster sizes considered. The insertion of metal atoms into small carbon rings significantly reduces the strain energy of the ring,[19] while the separation of the La atoms by carbon atoms reduces the electrostatic repulsion between the metal atoms carrying a partial positive charge. Structures where both metal atoms are a part of the ring also have calculated mobilities closest to the ones measured for $La_2C_n^+$ ($n = 0-6$) clusters.

The measured mobilities of $La_2C_7^+$ and the "slower" (smaller mobility) isomers of $La_2C_n^+$ ($n = 8-10$) deviate slightly from those calculated for planar $La_2C_n^+$ rings with two inserted metal atoms (see Figure 9). The strain energy associated with the formation of a ring decreases with the size of the ring, and so does the energy gain from insertion of a metal atom into the ring. Thus carbon rings with metal atoms attached to them (which have more carbon−carbon bonds) become energetically competitive. The mobilities of La-containing carbon rings with externally attached La atoms are slightly larger than those with inserted metal atoms.[17,19] For example, the calculated mobilities of planar $La_2C_9^+$ and $La_2C_{10}^+$ rings with one La atom inserted into the ring and the other one attached externally are in excellent agreement with those measured experimentally for "slower" $La_2C_n^+$ ($n = 9, 10$) isomers.

(34) Ross, R. B.; Powers, J. M.; Atashroo, T.; Ermler, W. C.; LaJohn, L. A.; Christiansen, P. A. *J. Chem. Phys.* **1990**, *93*, 6654.

(35) Frisch, M. J. *et al*., Gaussian-92, Revision E.1, Gaussian, Inc.: Pittsburg, PA, 1992.

(36) McElvany, S. W.; Dunlap, B. I.; O'Keefe, A. *J. Chem. Phys.* **1987**, *86*, 715.

(37) von Helden, G.; Gotts, N. G.; Maitre, P.; Bowers, M. T. *Chem. Phys. Lett.* **1994**, *227*, 601.

The growth pattern of $La_2C_n^+$ ($n = 17-26$) *rings* is markedly different from that characteristic of planar rings and observed for small $La_2C_n^+$ clusters. In this size range planar mono- and bicyclic rings are the only stable isomers observed for both C_n^+ and LaC_n^+ clusters.[15,19] However, the decrease in the mobilities of $La_2C_n^+$ ($n \geq 17$) *rings* with the addition of consecutive carbon atoms is much smaller than expected for planar ring structures, and slightly larger than expected for graphite sheets (see Figures 9 and 3). Planar polycyclic rings could give rise to the growth pattern observed for $La_2C_n^+$ ($n \geq 17$) *rings*, but they are expected to be too strained to be stable in this size range. A three-dimensional complex of two metal-containing carbon rings seems to be the most plausible structure for $La_2C_n^+$ ($n \geq 17$) *rings*. Of the possible spatial arrangements of two rings, a stack of roughly parallel rings of approximately equal size (such as the one pictured as structure **B** in Figure 9) is expected to give the smallest change in the mobility with increasing cluster size. Our mobility simulations show that the growth pattern corresponding to this structure (the dashed line in Figure 9) very closely resembles the one observed for $La_2C_n^+$ ($n \geq 17$) *rings*.

Several bonding arrangements can be proposed to rationalize the $La_2C_n^+$ geometry with two roughly parallel rings suggested by our mobility measurements. One of the plausible arrangements is presented in Figure 9 as structure **B**. The $La_2C_{16}^+$ cluster shown in this figure is comprised of two C_8 rings with inserted La atoms. The mutual orientation of the rings is chosen in such a way that their dipole moments are antiparallel. The geometry of this three-dimensional ring complex (as well as of similar complexes of several other sizes) has been optimized in quantum chemical calculations at the Hartree−Fock level (only the doublet structure has been considered). In the equilibrium geometry the metal atoms are displaced from the planes of the rings by about 1 Å and the rings themselves are slightly bent. The distance between the ring planes is around 3.8 Å. The dashed line in Figure 9 shows the mobilities calculated for similar structures over a range of cluster sizes. The agreement with the measured mobilities of $La_2C_n^+$ ($n \geq 17$) *rings* is excellent.

The stability of three-dimensional ring complexes similar to structure **B** is expected to be due largely to electrostatic interactions. Because of the low (5.58 eV[38]) ionization potential of La, La-containing carbon rings must have large dipole moments (around 5 D from our quantum chemical calculations for rings with around 10 atoms). The mutual orientation of La-containing rings in structure **B** ensures an electrostatic attraction between the rings. The displacement of metal atoms out of the ring planes further increases this attraction. In addition, $La_2C_n^+$ clusters have at least one unpaired electron, which can contribute to the bonding between rings through La(dπ)−C(pπ) orbital overlap. This type of interaction is known to produce very strong dπ−pπ chemical bonds in cyclopentadienyl compounds of lanthanides (3.73 eV for the La−C_5H_5 bond in $La(C_5H_5)_3$[39]). Our dissociation energy measurements (Table 2) do suggest that three-dimensional $La_2C_n^+$ ring complexes are fairly strongly bound.

The electrostatic interactions are also likely to be the driving force for the formation of three-dimensional $La_2C_n^+$ ring complexes. One of the pathways for the formation of $La_2C_n^+$ clusters, $LaC_{n-m}^+ + LaC_m \rightarrow La_2C_n^+$, involves a long-range ion−dipole attraction of two metal-containing carbon clusters. This attraction should drive the formation of complexes similar to structure **B** without, or with very small, activation barriers, making these complexes the kinetically favored species. The observation that upon collisional excitation three-dimensional $La_2C_n^+$ ring complexes do not convert into planar ring structures either directly or after dissociation implies that they may be favored not only kinetically but also thermodynamically.

In order to minimize the strain energy, small three-dimensional ring complexes must consist of rings of approximately equal size. Thus only a small group of closely shaped isomers should form, as is observed for $La_2C_n^+$ ($n < 25$) clusters. As the rings grow larger, the role of the strain energy decreases and the shapes of the rings may become more diverse. The formation of three-dimensional complexes of rings of various sizes can account for the broadening of the *ring* peak in the drift time distributions of $La_2C_n^+$ ($n \geq 25$) clusters (see Figure 2). For even larger clusters, three-dimensional complexes of bi- and polycyclic La-containing rings can form, so that the isomer distribution becomes extremely broad (Figure 2).

Despite the good agreement between the mobilities measured for $La_2C_n^+$ ($n \geq 17$) *rings* and those calculated for structure **B**, we cannot be certain about this structural assignment. Other structures with similar mobilities almost certainly exist. However, the data presented in Figure 9 clearly indicate that large $La_2C_n^+$ *rings* are not planar ring structures and are thus substantially different from C_n^+ and LaC_n^+ ring isomers. We are certain about our general assignment of $La_2C_n^+$ *rings* to three-dimensional ring complexes. A more detailed structural description is unavoidably more speculative, although our mobility simulations do suggest that the three-dimensional $La_2C_n^+$ ring complex must resemble structure **B**.

The inverse mobilities of $La_2C_n^+$ ($n = 11-16$) *rings* and the "faster" isomer of $La_2C_n^+$ ($n = 8-10$) *rings* do not exhibit a well-defined growth pattern. Planar ring structures with mobilities close to the measured ones can be suggested in this size range. For example, the "faster" $La_2C_n^+$ ($n = 8-10$) *ring* isomer can be attributed to a planar carbon ring with one metal atom inserted into the ring and another one bound inside the ring, similar to the structure proposed to explain one of the LaC_n^+ ring isomers.[19] On the other hand, the mobilities measured for this isomer are in excellent agreement with those calculated for structure **B** (See Figure 9). Since three-dimensional ring complexes and certain planar ring structures may have similar mobilities in the $n = 8-16$ size range, their coexistence will not lead to a significant broadening of the peaks in the drift time distributions (See Figure 2). The exact cluster size where planar ring growth gives way to three-dimensional growth is not clear from our data.

(d) The Fullerene+Ring Family. The broad *fullerene+ring* distribution of isomers gradually appears in the place of the *fullerene I* structure as the cluster size increases (see Figure 1b−e). This suggests that there is a certain structural similarity between *fullerenes+rings* and fullerenes. Large C_n^+ and LaC_n^+ clusters formed by laser vaporization show a strong tendency to form fullerenes[15,19] (see Figure 4d,e), and the relative abundance of fullerenes in these systems always increases with the cluster size. Thus the *fullerene+ring* isomers are probably fullerene derivatives. Since small LaC_n^+ and $La_2C_n^+$ clusters are metal-containing carbon rings, it is reasonable to assume that a fullerene and a ring can fuse to form fullerene+ring complexes. The mobilities of such structures should vary widely with the relative size of the fullerene and the ring, explaining the large width of the *fullerene+ring* peak in the drift time distributions. Mobility simulations show that the mobility dependence observed for the center of the *fullerenes+rings* peak (the open circles in Figure 3) would correspond to an *n*-atom cluster consisting of a fullerene with about 4*n*/5 atoms and a ring with about *n*/5 atoms, if the fullerene+ring complex is formed through a [2 + 2] cycloaddition. Similar structures have

(38) *CRC Handbook of Chemistry and Physics*, 63rd ed.; CRC Press: Boca Raton, FL, 1984.

(39) Devyatykh, C. G.; Rabinovich, I. B.; Tel'noi, V. I.; Borisov, G. K.; Zyazina, L. F. *Dokl. Akad. Nauk SSSR* **1974**, *217*, 673.

been proposed to explain the low-intensity features in the drift time distributions of large (100−300 atoms) C_n^+ clusters.[40] However, in the C_n^+ system the fullerene+ring isomers are less abundant than the regular fullerenes, while *fullerenes+rings* are the dominant isomer in the unannealed drift time distributions of large $La_2C_n^+$ clusters. Thus it seems that the presence of the metal atoms plays an important role in the stabilization of fullerene+ring complexes or somehow assists in their formation. For example, a fullerene and a ring can be brought together by an ion−dipole attraction and form an electrostatically bound complex, as discussed above for $La_2C_n^+$ *rings*. Alternatively, a complex of a $La_2C_n^+$ fullerene with one non-endohedral metal atom and a carbon ring may result from the interaction between the ring and the non-endohedral metal atom.

Planar rings and fullerenes are the most abundant species observed for LaC_n^+ clusters.[19] A fusion of these isomers can render ring+ring, fullerene+ring, and fullerene+fullerene complexes. As described above, the first two complexes are rather abundant for $La_2C_n^+$ clusters. There are physical reasons to expect fullerene+fullerene complexes (fullerene dimers or "peanuts"[41]) to form as well. Endohedral $M_2@C_n$ fullerenes (especially the smaller ones) are destabilized by the electrostatic repulsion between the metal atoms, both of which are expected to donate significant electron density to the carbon cage.[42] The formation of a complex of two smaller endohedral fullerenes reduces this repulsion, although at the expense of strain energy. Our mobility simulations show that the inverse mobilities of fullerene dimers should parallel those of regular fullerenes. The difference between the mobilities of fullerene dimers and regular fullerenes of the same size depends on the intershell distance of the dimer and is 12−14% for an intershell distance of 2.9 Å (as estimated for C_{60} dimers formed through the laser ablation of fullerene films[43]). A part of the broad *fullerene+ring* isomer distribution may be due to fullerene dimers, although fullerene dimers alone cannot account for the entire *fullerene+ring* peak. Even if fullerene dimers exist at low injection energies, they do not survive the collisional heating process, and we observe no dissociation fragments attributable to these species.

2. Fullerene Formation. Our previous studies of LaC_n^+,[18,19] NbC_n^+,[20] and ZrC_n^+ [44] clusters have shown that planar carbon rings containing these metals start to efficiently isomerize into fullerenes at much smaller cluster sizes than pure carbon rings. In the metal−carbon systems, fullerenes become the dominant isomer for clusters with around 35 carbon atoms, while they are only a minor isomer for C_n^+ clusters of this size. The increased efficiency of fullerene formation in these systems, however, does not seem to be related to the lowering of the activation energies for the ring-to-fullerene isomerization. For LaC_n^+ and NbC_{2n}^+ rings the activation energies are close to or slightly larger than those for C_n^+ rings, while for ZrC_n^+ and NbC_{2n+1}^+ rings they are lower by about 0.5−0.7 eV.

The activation energies for the isomerization of three-dimensional $La_2C_n^+$ ring complexes into metallofullerenes are about 1 eV lower than those observed for the isomerization of planar C_n^+ and LaC_n^+ rings (see Table 1). This substantial reduction may be related to the differences in the shapes of the reactants (three-dimensional versus planar rings) or to the presence of the second metal atom. Generally, transition metal atoms are expected to be able to reduce the activation energies for the cross-linking of carbon chains involved in ring-to-fullerene isomerization. The inability of a single La atom to lower the activation energy has been attributed to the lack of nonbonding valence electrons.[19] In the $La_2C_n^+$ system there is at least one unpaired electron, and it is likely to be localized on one of the metal atoms. In this respect the $La_2C_n^+$ system is similar to the ZrC_n^+ system, where the activation energies for planar rings-to-fullerenes isomerization are about 0.7 eV lower than in the C_n^+ and LaC_n^+ systems, but still higher than those observed in the $La_2C_n^+$ system. Thus it is possible that the three-dimensional arrangement of metal-containing rings aids in their isomerization into fullerenes.

The experimental data on the isomerization of pure C_n^+ rings into fullerenes suggest that the activation energy for this process is determined by the first few steps of the reaction, which have been associated with the formation of radical intermediates and the buildup of the strain energy.[22] Thus it is not unexpected that the activation energy may be quite sensitive to the initial geometry of a cluster. For example, in the fullerene formation mechanism proposed by Hunter *et al.*[22] the rate-determining step is the retro-[2 + 2] process (with an activation energy around 2.7 eV[45]), necessitated by the presence of a [2 + 2] junction in the bicyclic ring reactant. If such defects were not present in the reactant, the ring-to-fullerene conversion could proceed through a series of Bergman cyclizations (activation energy around 1.4 eV[46]) and radical-induced cross-linkings[22,47] with the activation energies of 1 eV or less (in the absence of strain). It is possible that the initial stack-like spatial arrangement of the rings allows them to "choose" the type of junction they may form, avoiding the formation of defect-containing intermediates in the early stages of the isomerization, so that the reaction can proceed along this low activation energy pathway.

Conclusions

The growth sequence typical for medium-sized pure carbon clusters and carbon clusters containing a single metal atom (association of pure and metal-containing carbon rings into covalently bound planar complexes with the possibility of subsequent isomerization into fullerenes or graphite sheets) is substantially altered by the presence of a second metal atom. The growth of $La_2C_n^+$ clusters seems to proceed through the association of two metal-containing fragments (presumably through the formation of La−C bonds), resulting in the new classes of isomers, such as three-dimensional ring+ring and fullerene+ring complexes. An ion−dipole interaction between metal-containing carbon clusters may play an important role in this process, allowing the formation of electrostatically bound precursors and/or products. The results of the present work lead one to predict that rather complicated structures, such as ring+ring+ring or fullerene+ring+ring complexes, may be formed for carbon clusters containing three and more metal atoms. Another unexpected result of the present work is the dramatic lowering of the activation barriers for the isomerization of rings into fullerenes observed in the $La_2C_n^+$ system. This lowering may be due to the catalytic effect of the metal atoms on the cross-linking of carbon chains or to the nonplanar arrangements of the carbon rings in the reactants.

Acknowledgment. We gratefully acknowledge the support of this work by the National Science Foundation (Grant No. CHE-9306900) and the donors of the Petroleum Research Fund (administered by the American Chemical Society).

JA953071K

(40) Hunter, J. M.; Jarrold, M. F. *J. Am. Chem. Soc.* In press.
(41) Strout, D. L.; Murry, R. L.; Xu, C.; Eckoff, W. C.; Odom, G. K.; Scuseria, G. E. *Chem. Phys. Lett.* **1993**, *214*, 576.
(42) Nagase, S.; Kobayashi, K. *Chem. Phys. Lett.* **1994**, *231*, 319.
(43) Hunter, J. M.; Fye, J. L.; Boivin, N. M.; Jarrold, M. F. *J. Phys. Chem.* **1994**, *98*, 7440.
(44) Shelimov, K. B.; Jarrold, M. F. Unpublished results.
(45) Chesick, J. P. *J. Phys. Chem.* **1961**, *65*, 2170.
(46) Bergman, R. G. *Acc. Chem. Res.* **1973**, *6*, 25.
(47) Schweigert, V. A.; Alexandrov, A. L.; Morokov, Y. N.; Bedanov, V. M. *Chem. Phys. Lett.* **1995**, *235*, 221.